**PAPER**

# A conjugated polymer based on 5,5′-bibenzo[c][1,2,5]thiadiazole for high-performance solar cells†

Haifeng Wang,[ab] Pei Cheng,[ab] Yao Liu,[ab] Jianming Chen,[ab] Xiaowei Zhan,*[a] Wenping Hu,[a] Zhigang Shuai,[a] Yongfang Li[a] and Daoben Zhu[a]

Based on a new n-type building block 5,5′-bibenzo[c][1,2,5]thiadiazole (BBT), we designed and synthesized a carbazole–BBT D–A copolymer (**P1**), and compared it with its carbazole–benzo[c][1,2,5]thiadiazole (BT) analog **P2**. **P1** has good solubility in common organic solvents, while **P2** has poor solubility. In films, **P1** and **P2** exhibit absorption maxima at 565 and 614 nm, respectively. The HOMO level of **P1** is −5.51 eV, 0.18 eV lower than that of **P2**, while the LUMO level of **P1** is −3.56 eV, slightly lower than that of **P2**. The low-lying energy levels and blue-shifted absorption of **P1** are attributed to the stronger electron-withdrawing ability of BBT and the twisted main chain of **P1**. The field-effect hole mobility of **P1** is $2 \times 10^{-3}$ cm² V⁻¹ s⁻¹. Polymer solar cells based on **P1**:PC₇₁BM (1 : 3, w/w) exhibit a power conversion efficiency up to 3.7% with a high open circuit voltage of 0.98 V under an AM 1.5 simulated solar light at 100 mW cm⁻².

## Introduction

Since the discovery of photoinduced charge transfer in composites of conjugated polymers and C₆₀,[1] polymer solar cells (PSCs) have attracted considerable attention because they have shown promising potential as a result of their unique advantages such as low cost, light weight and large-area fabrication on flexible substrates.[2] The achieved power conversion efficiencies (PCEs) have evolved from less than 1% in poly(phenylene vinylene) (PPV)/PC₆₁BM in 1995,[3] to 4–5% in poly(3-hexylthiophene) (P3HT)/PC₆₁BM in 2005,[4] now to over 7% in benzodithiophene-based copolymers.[5] However, the efficiencies of the PSCs are still far below 10% that is often regarded as being a prerequisite for large-scale commercial applications.

To achieve high performance of PSCs, the properties of the polymers are very important. Ideally, the polymers should have a low band gap to ensure efficient harvesting of the solar photons and high charge carrier mobility for charge transport, which will guarantee a high short-circuit current density ($J_{sc}$). Furthermore, the highest occupied molecular orbital (HOMO) of the polymers should be low, which will enhance the open-circuit voltage ($V_{oc}$) since $V_{oc}$ is closely related to the offset between the energy levels of the HOMO of the donor and the lowest unoccupied molecular orbital (LUMO) of the acceptor.[6] Over the past decade, high $J_{sc}$

of PSCs have been achieved with low-band-gap polymers, however, some of them gave low PCEs owing to the low $V_{oc}$ of 0.3–0.5 V.[7] On the other hand, some kinds of polymers, such as polyfluorene and its derivatives, showed low HOMO levels and gave high $V_{oc}$, while their wide band gaps resulted in low $J_{sc}$ and low efficiencies.[8] To enhance the efficiency, polymer donors should have a low band gap and low HOMO. The donor–acceptor (D–A) strategy has been demonstrated to be powerful in not only band-gap engineering but also tuning of the energy levels of the HOMOs and LUMOs.[9]

Among the acceptor building blocks, benzo[c][1,2,5]thiadiazole (BT) is commonly used for designing D–A type polymers due to its strong electron-withdrawing ability and the existence of the heteroatom interactions.[10] Copolymers of BT with various donor units, such as fluorene, silafluorene, indolo[3,2-b]carbazole, pentacyclic fused thiophene–phenylene–thiophene, dithienocyclopentadiene, dithienosilole, dithienopyrrole, and benzodithiophene, have shown promising photovoltaic performance with PCEs of 2–6%.[11] Very recently, Wang *et al.* reported the use of naphtho[1,2-c:5,6-c]bis[1,2,5]-thiadiazole (NT) as a new acceptor unit in D–A conjugated polymers for high-performance PSCs.[12]

Poly(2,7-carbazole)s are excellent candidates for polymer solar cells owing to their easily modulated physical properties and electron-rich characteristics. Initial studies by Müllen, Leclerc and coworkers reported that PSCs based on poly(2,7-carbazole) derivatives exhibited PCEs of 0.6–0.8%.[13] Later on, through incorporating an electron-accepting unit such as BT, Leclerc and coworkers developed a series of D–A type poly(2,7-carbazole)-based polymers, among which, a carbazole–BT copolymer exhibited the best PCE of 3.6%.[14,15] When replacing PC₆₁BM

*[a]Beijing National Laboratory for Molecular Sciences and Institute of Chemistry, Chinese Academy of Sciences, Beijing, 100190, China. E-mail: xwzhan@iccas.ac.cn*
*[b]Graduate University of Chinese Academy of Sciences, Beijing, 100049, China*
† Electronic supplementary information (ESI) available: ¹H NMR spectra for BBT and its dibromides. See DOI: 10.1039/c2jm14283j

with $PC_{71}BM$ together with titanium oxide as the optical spacer and hole blocking layer, Heeger and coworkers improved the PCE to 6.1%.[16] Bo *et al.* reported an analogue of carbazole–BT copolymer with dioctoxy groups on BT giving a PCE of 5.4% in combination with $PC_{71}BM$.[17] Although the carbazole–BT copolymers afforded high performance in PSCs, in some cases they suffer from limited solubility at room temperature due to the planar polymer backbone and the strong interchain interaction, which will cause inconvenience in characterization and device fabrication.[17]

We are interested in 5,5′-bibenzo[c][1,2,5]thiadiazole (BBT), which is a 5,5′-connected dimer of BT. There has been only one report[18] for BBT synthesis but no report regarding its use in the synthesis of organic semiconductors. Relative to BT, BBT has a stronger electron-accepting ability due to two BT units, facilitating the manipulation of the electronic structure (HOMO/LUMO levels and band gap). On the other hand, BBT tends to adopt a twisted geometry due to the steric hindrance between the two BT components, which leads to weaker intermolecular interaction and better solubility. Furthermore, four amendable reactive positions endow BBT with easy molecular structure tailoring. Therefore, BBT could be a promising n-type building block for synthesizing organic semiconductors. In this contribution, we designed and synthesized a carbazole–BBT D–A copolymer (**P1**, Fig. 1), and compared with its carbazole–BT analog **P2**. Relative to **P2**, **P1** exhibits better solubility and a lower HOMO level. **P1** exhibits a hole mobility of $2.0 \times 10^{-3}$ $cm^2$ $V^{-1}$ $s^{-1}$. PSCs based on **P1**:$PC_{71}BM$ exhibit $V_{oc}$ as high as 0.98 V and PCEs as high as 3.7% without device optimization and post-treatments.

## Results and discussion

### Synthesis and characterization

The synthetic routes for the monomers and polymers are outlined in Scheme 1. To ensure good solubility, a long and branched 2-decyl-tetradecyl group was attached onto 2,7-dibromocarbazole to form compound **1**. Stille coupling reaction of **1** with thiophene tin gave rise to **2**, which was treated with n-BuLi and then $SnMe_3Cl$ to form monomer **3**. 5,5′-Bibenzo[c][1,2,5]thiadiazole (BBT) was synthesized according to the literature.[18] The key monomer **4** was synthesized by treating BBT with $HBr/Br_2$. Bromination of BBT gave a mixture of mono-, di-, tri-, and tetrabromide of BBT, which can be separated by column chromatography. However, BBT dibromide could have 4 possible isomers (Fig. S1,† ESI), which cannot be separated by column chromatography (Figure S3,† ESI). Thus, the isomer mixture was further treated with $Br_2$ in HBr solution (1 : 5 molar ratio). Probably due to the dominated ratio in the mixture (Figure S3,† ESI) and relatively weaker reactivity of **4**, isomers
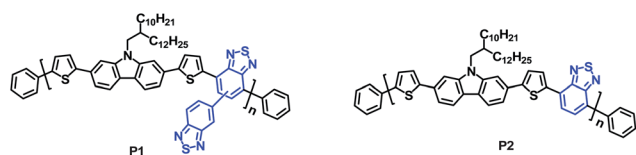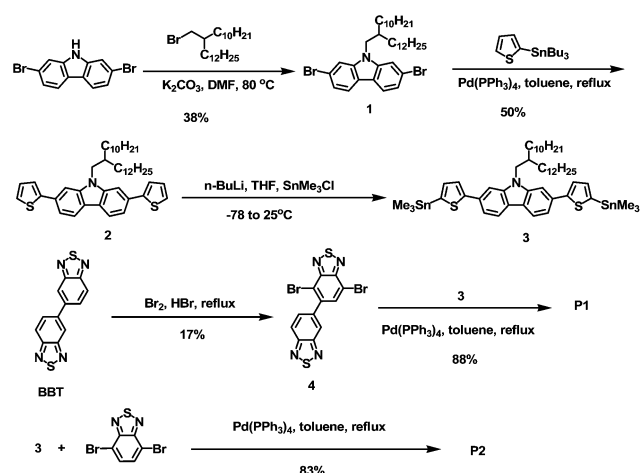
**Scheme 1** Synthetic routes for the monomers and polymers.

**4a–c** were completely converted to tri- and tetrabromide while most of **4** still remained. Finally the pure isomer **4** was isolated by column chromatography and fully characterized by NMR, HRMS and elemental analysis. To obtain enough amount of **4**, this reaction was run three times with good reproducibility (yields 15–20%). The $^1H$ NMR spectrum of the isolated compound clearly demonstrates that its chemical structure is **4** other than **4a–c** (Fig. S4,† ESI). Stille coupling of **3** with **4** or 4,7-dibromobenzo[c][1,2,5]thiadiazole afforded **P1** and **P2**, respectively.

**P1** has good solubility in common organic solvents, such as $CHCl_3$ and *o*-dichlorobenzene. However, **P2** has poor solubility even in different solvents such as $CHCl_3$, THF, chlorobenzene and *o*-dichlorobenzene *etc* or at high temperatures (>100 °C). To our surprise, **P2** has the same main chain but different side chain compared to the carbazole–BT copolymer **PCDTBT** reported by Leclerc and coworkers,[15] but their solubility is different: **P2** with longer side chains has poor solubility while **PCDTBT** with shorter side chains has good solubility. The difference in solubility of **P2** and **PCDTBT** may be related to the side chains and/or molecular weights. **P1** has a number average molecular weight ($M_n$) of 12 000, a weight average molecular weight ($M_w$) of 29 000, and a polydispersity index of 2.5. Considering the polymerization time for **P2** (24 h) is shorter than that (72 h) for **P1**, **P2** possibly has a similar or even smaller molecular weight than **P1**. While **PCDTBT** has a $M_n$ of 37 000 and a $M_w$ of 73 000,[15] much higher than **P1** and **P2**. So polymer molecular weight is probably not a key factor for the difference in solubility of **P2** and **PCDTBT**. The poor solubility of **P2** may be due to its more planar polymer backbone and stronger interchain interaction (see following theory calculation and optical properties parts). Thermogravimetric analysis (TGA) shows that **P1** has excellent thermal stability with a 5% loss temperature of 415 °C under nitrogen (Fig. 2).

### Theoretical calculation

To provide an insight into the molecular architecture of the polymers, molecular simulation was carried out for **P1** and **P2** with a chain length of $n = 1$ using density functional theory
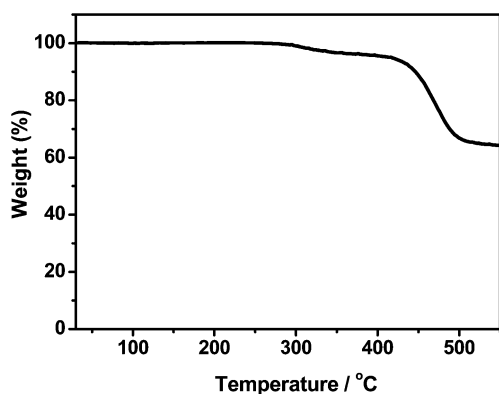
**Fig. 1** The chemical structure of **P1** and **P2**.

**Fig. 2** The TGA curve of **P1**.



**Fig. 4** The molecular orbital geometry and energy levels obtained from DFT calculations on **P1** and **P2** with a chain length $n = 1$ at the B3LYP/6-31G* level.

(DFT) at the B3LYP/6-31G(d,p) level[19,20] with the Gaussian 09 program package.[21] Since the BBT unit is asymmetric, the repeat unit of **P1** has two regiochemical isomers. To simplify the calculation, we just select one isomer as a theory model (Fig. 3). Dihedral angles between carbazole and thiophene ($D_1$) are almost same for **P1** and **P2**. However, the dihedral angle between thiophene and BBT ($D_2$) in **P1** is 43.8°, much larger than that (6°) between thiophene and BT ($D_2$) in **P2**. The dihedral angle between two BT in BBT ($D_4$) in **P1** is very large (56.9°). Thus, **P1** has a more twisted main chain, while **P2** has a more planar main chain. The more twisted conformation of the main chain leads to weaker interchain interaction and better solubility of **P1**.

Fig. 4 shows the calculated molecular orbital geometry and energy levels of the polymers. For **P1** and **P2**, the HOMOs are delocalized over the polymer backbones, while the LUMOs are located on the BBT or BT unit. Relative to **P2**, **P1** has a lower HOMO due to the twisted main chain and relatively localized HOMO, and has a lower LUMO as a result of the stronger electron-withdrawing ability of BBT unit.
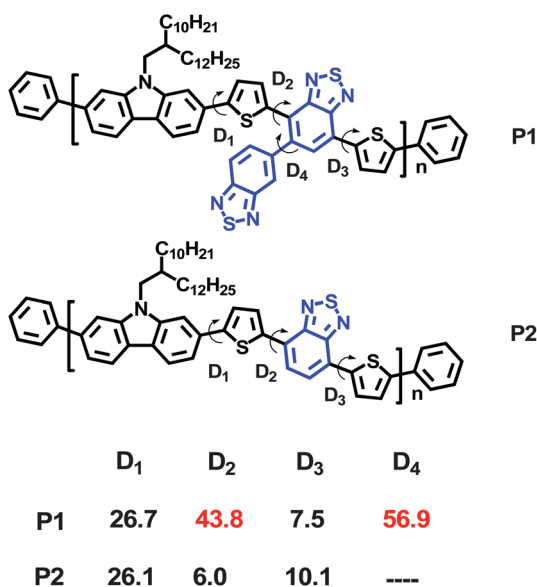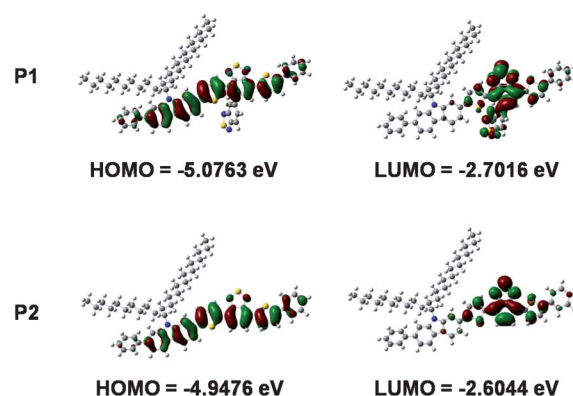
## Optical properties

UV-vis absorption spectra of **P1** and **P2** were measured in CHCl₃ ($ca.$ $10^{-6}$ M) solution and in thin films (Fig. 5), and the results are summarized in Table 1. In solution, **P1** exhibits an absorption maximum at 531 nm, while **P2** exhibits an absorption maximum at 546 nm with a shoulder at $ca.$ 607 nm. In film, the absorbance maximum of **P1** is 565 nm, a 34 nm red shift relative to that in solution. **P2** exhibits red-shifted absorption and the shoulder peak enhances to a maximum peak. The red-shifted absorption of **P2** relative to **P1** is attributed to the more planar backbone. The strong shoulder peak of **P2** suggests the strong interchain interaction due to the planar structure of the main chain in **P2**.

Interestingly, **P2** has the same main chain but different side chain compared to the carbazole–BT copolymer **PCDTBT** reported by Leclerc and coworkers,[15] but their absorption spectra are different. **P2** exhibits an absorption maximum at 614 nm with a distinct shoulder peak in film and a band gap of 1.8 eV, while **PCDTBT** exhibits an absorption maximum at 576 nm without a shoulder peak in film and a band gap of 1.88 eV. On the other hand, **P2** with longer side chains has poor solubility while **PCDTBT** with shorter side chains has good solubility. The red-shifted absorption with shoulder peak and poor solubility of **P2** suggests stronger interchain interaction relative to **PCDTBT**. Thus, the 2-decyl-tetradecyl side chain in **P2** seems to facilitate



| | $D_1$ | $D_2$ | $D_3$ | $D_4$ |
|---|---|---|---|---|
| **P1** | 26.7 | 43.8 | 7.5 | 56.9 |
| **P2** | 26.1 | 6.0 | 10.1 | ---- |

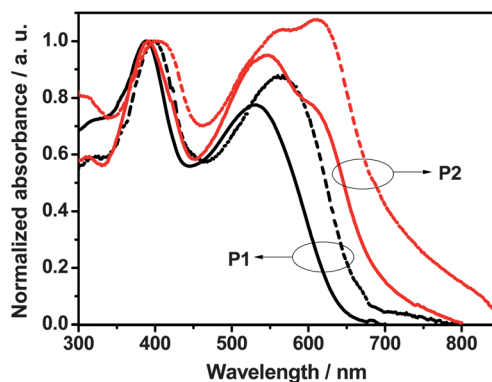**Fig. 3** Several key dihedral angles of the polymers.



**Fig. 5** Absorption spectra of **P1** and **P2** in solution (solid) and in film (dash).

**Table 1** The optical and electrochemical properties of **P1** and **P2**

| | $\lambda_{abs}^{a}$/nm | $E_{g}^{opt\ b}$/eV | HOMO$^{c}$/eV | LUMO$^{c}$/eV | $E_{g}^{cv\ d}$/eV |
|---|---|---|---|---|---|
| **P1** | 531 (565) | 1.88 | −5.51 | −3.56 | 1.95 |
| **P2** | 546 (614) | 1.80 | −5.33 | −3.51 | 1.82 |

[a] Measured in chloroform; data in thin films are given in the parentheses. [b] Estimated from the onset edge of absorption in film. [c] Estimated from the onset oxidation and reduction potentials, respectively, assuming the absolute energy level of ferrocene/ferrocenium (Fc/Fc$^{+}$) to be 4.8 eV under vacuum. [d] HOMO–LUMO gap estimated from electrochemistry.

molecular self-assembly compared to the 1-octyl-nonyl side chain in **PCDTBT**.

## Electrochemical properties

To investigate the electrochemical properties of the polymers and estimated their HOMO and LUMO energy levels, cyclic voltammetry (CV) was carried out using glassy-carbon coated with polymer films, a Pt wire and an Ag wire coated with AgCl as the working electrode, counter electrode, and quasi-reference electrode, respectively. CV measurements were conducted in a 0.1 M Bu$_4$NPF$_6$ acetonitrile solution under N$_2$ at a scan rate of 50 mV s$^{-1}$. Fig. 6 shows CV curves of **P1** and **P2**. The HOMOs and LUMOs were estimated from the onset oxidation and reduction potentials, assuming the absolute energy level of ferrocene/ferrocenium to be 4.8 eV under vacuum, and the data are summarized in Table 1. The HOMO level of **P1** is −5.51 eV, 0.18 eV lower than that of **P2**, which is attributed to the stronger electron-accepting ability of BBT and the twisted main chain of **P1**. The LUMO level of **P1** is −3.56 eV, slightly lower than that of **P2**. The electrochemistry data are in considerable agreement with calculation results. The HOMO–LUMO gap ($E_{g}^{cv}$) of **P1** (1.95 eV) is larger than that of **P2** (1.82 eV), which corresponds well with the optical bandgaps, $E_{g}^{opt}$.

## Organic field-effect transistors

To ensure effective charge carrier transport to the electrodes and to reduce the photocurrent loss in solar cells, high mobility is a basic
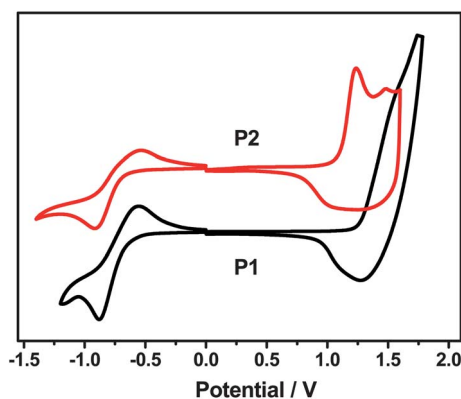
requirement for effective photovoltaic polymers. To measure mobilities of the polymers, organic field-effect transistors (OFETs) based on **P1** were fabricated on octadecyltrichlorosilane (OTS)-treated SiO$_2$/Si substrates through a spin-coating process in a top contact geometry using Au as the source and drain electrodes. **P2** can not be used to fabricate OFETs due to its poor solubility. **P1** exhibited typical p-type semiconductor behavior in air (Fig. 7) with a mobility of $2 \times 10^{-3}$ cm$^2$ V$^{-1}$ s$^{-1}$ ($V_{th} = -18$ V, $I_{on}/I_{off} = 10^4$), which is similar to those of BT-based poly(2,7-carbazole) derivatives.[14,17]

## Polymer solar cells

To demonstrate the potential application of **P1** in polymer solar cells (PSCs), we used **P1** as an electron donor and PC$_{71}$BM[22] as an electron acceptor, and fabricated bulk heterojunction PSCs with a structure of ITO/PEDOT:PSS/**P1**:PC$_{71}$BM(1 : 3, w/w)/Al. **P2** can not be used to fabricate PSCs due to its poor solubility. Photovoltaic cells, when tested under an AM 1.5 solar illumination at 100 mW cm$^{-2}$ source intensity, demonstrated the best PCE of 3.7% with a good short-circuit current density ($J_{sc} = 9.2$ mA cm$^{-2}$) and a high open-circuit voltage ($V_{oc} = 0.98$ V) (Fig. 8). More than 20 devices were fabricated and their average PCEs were 3.61%. The $V_{oc}$ value is higher than that (0.81–0.86 V) of BT-based poly(2,7-carbazole)s devices due to the lower HOMO of **P1**.[14,17] However, the fill factor ($FF = 41\%$) is lower compared to that (up to 69%) of BT-based poly(2,7-carbazole)s devices.[14–17]





**Fig. 6** Cyclic voltammograms of **P1** and **P2** in CH$_3$CN/0.1 M [$^n$Bu$_4$N]$^+$[PF$_6$]$^-$ at 50 mV s$^{-1}$. The horizontal scale refers to an anodized Ag wire pseudo-reference electrode. The oxidation potential of ferrocene *versus* Ag wire is 0.55 V.
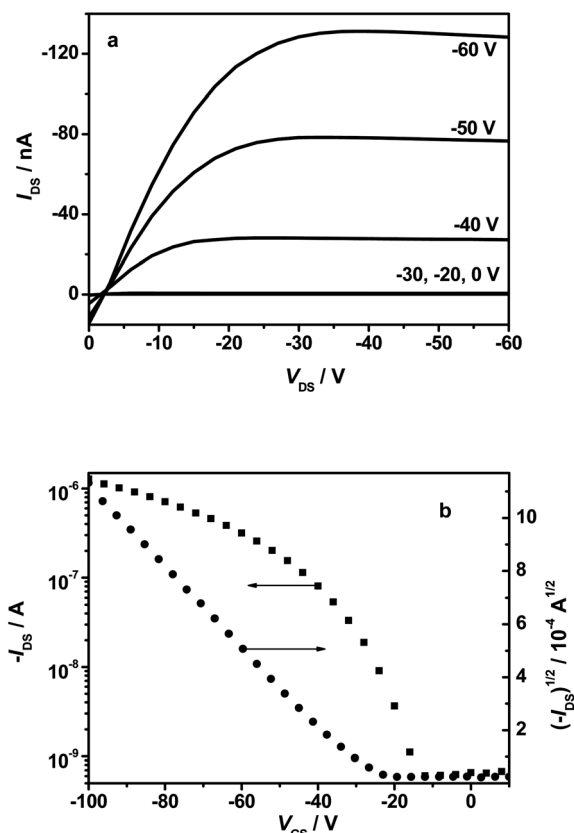
**Fig. 7** Typical current–voltage characteristics ($I_{DS}$ *vs.* $V_{DS}$) at different gate voltages ($V_{GS}$) (a) and $-I_{DS}$ and $(-I_{DS})^{1/2}$ *vs.* $V_{GS}$ plots at $V_{DS}$ of −100 V (b) for a top contact device based on **P1**.

This journal is © The Royal Society of Chemistry 2012

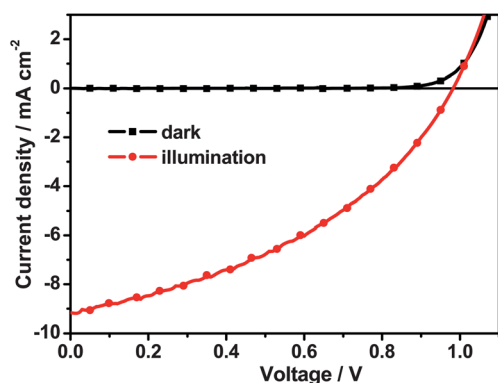*J. Mater. Chem.*, 2012, **22**, 3432–3439 | 3435

**Fig. 8** The current density–voltage characteristics of a device with the structure of ITO/PEDOT:PSS/**P1**:PC$_{71}$BM(1 : 3, w/w)/Al.

As shown in Fig. 9, the device based on **P1**:PC$_{71}$BM (1 : 3, w/w) exhibits a broad external quantum efficiency (EQE) plateau with the maximum EQE of 52% at 492 nm. It is worth noting that the performance of **P1**-based solar cells was obtained without any post-treatments, *e.g.* thermal annealing, solvent annealing or additive addition. Optimization of the device structures and post-treatments can be expected to substantially increase the PCE of the PSCs.

The film morphology of the **P1**:PC$_{71}$BM (1 : 3, w/w) blend was examined by atomic force microscopy (AFM) in tapping mode. The film exhibits a typical cluster structure with many aggregated domains and a root-mean-square (RMS) roughness of 0.57 nm (Fig. 10a). The phase separation sizes estimated by cross-section profiles are about tens nanometres (Fig. 10b). This nanoscale phase separation is beneficial to exciton dissociation, charge transport and enhanced efficiency of the PSC.[23]

## Conclusions

Based on a novel n-type building block 5,5′-bibenzo[c][1,2,5] thiadiazole (BBT), we designed and synthesized a carbazole–BBT D–A copolymer (**P1**), and compared it with its carbazole-benzo[c][1,2,5]thiadiazole (BT) analog **P2**. Due to the twisted structure of BBT, the interchain interaction of **P1** is weaker, thus, **P1** has better solubility and a narrower absorption band than **P2**.
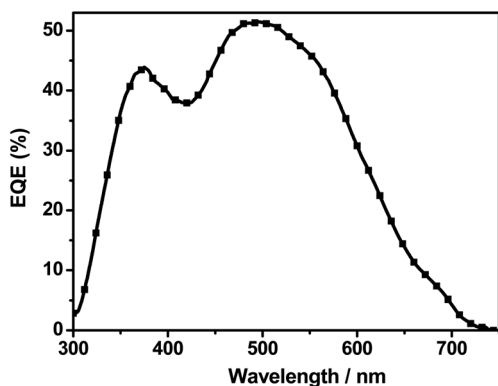


**Fig. 9** The EQE of **P1**:PC$_{71}$BM(1 : 3, w/w) film as a function of wavelength under the illumination of an AM 1.5 solar simulator, 100 mW cm$^{-2}$.
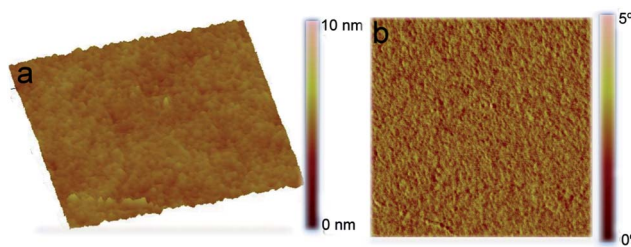


**Fig. 10** AFM height (a) and phase (b) images of the **P1**:PC$_{71}$BM (1 : 3, w/w) active layer in polymer solar cells. The graph size is 1 μm × 1 μm.

Due to the stronger electron-withdrawing ability of BBT and the twisted main chain, **P1** has a lower HOMO level relative to **P2**. The field-effect hole mobility of **P1** is 2 × 10$^{-3}$ cm$^2$ V$^{-1}$ s$^{-1}$, similar to that of BT-based poly(2,7-carbazole) derivatives. Under AM 1.5, 100 mW cm$^{-2}$, the polymer solar cells based on **P1**:PC$_{71}$BM (1 : 3, w/w) exhibit a power conversion efficiency of 3.7% and a high open-circuit voltage ($V_{oc}$) of 0.98 V without any post-treatments. Optimization of the device structures and post-treatments (*e.g.* thermal annealing, solvent annealing or additive addition) can be expected to substantially increase the PCE of the PSCs.

## Experimental section

### Materials

Unless stated otherwise, starting materials were obtained from Aldrich or Acros and were used without further purification. THF and toluene were distilled from sodium benzophenone under nitrogen prior to use. 5,5′-Bibenzo[c][1,2,5]thiadiazole (BBT) was synthesized according to the literature.[18]

### Characterization

The $^1$H and $^{13}$C NMR spectra were measured on a Bruker AVANCE 400 spectrometer. Mass spectra were measured on a GCT-MS micromass spectrometer using EI mode or on a Bruker Daltonics BIFLEX III MALDI-TOF Analyzer using MALDI mode. Elemental analyses were carried out using a FLASH EA1112 elemental analyzer. Solution (chloroform) and thin-film (on quartz substrate) UV-vis absorption spectra were recorded on a JASCO V-570 spectrophotometer. Electrochemical measurements were carried out under nitrogen on a deoxygenated solution of tetra-*n*-butylammonium hexa-fluorophosphate (0.1 M) in CH$_3$CN using a computer-controlled CHI660 electrochemical workstation, a glassy-carbon working electrode coated with polymer films, a platinum-wire auxiliary electrode, and an Ag wire anodized with AgCl as a pseudo-reference electrode. Thermogravimetric analysis (TGA) measurements were performed on Shimadzu thermogravimetric analyzer (model DTG-60) under a nitrogen flow at a heating rate of 10 °C min$^{-1}$. The GPC measurements were performed on a Waters 515 chromatograph connected to a Waters 2410 refractive index detector, using THF as eluent and polystyrene standards as calibrants, three Waters Styragel columns (HT3, 5, 6*E*) connected in series were used. The film morphology was analyzed in air using a Nanoscope III atomic force microscope (Digital Instruments) operated in tapping mode.

## Fabrication and characterization of organic field-effect transistors

Field-effect transistors based on **P1** polymer films were fabricated in the bottom gate, top contact configuration at ambient atmosphere. Highly n-doped silicon and thermally grown silicon dioxide (500 nm) were used as back gate and gate dielectric, respectively. The substrates were cleaned with pure water, hot concentrated sulfuric acid–hydrogen peroxide solution (concentrated sulfuric acid/hydrogen peroxide water = 2 : 1), pure water, and pure isopropyl alcohol. Then vaporized octadecyltrichlorosilane (OTS) was used for surface modification of the gate dielectric layer. Solutions of polymer in chloroform (about 5 mg mL$^{-1}$) were spin coated onto OTS-treated substrates to form thin polymer films. Gold contacts (25 nm) for source and drain electrodes were vacuum-deposited at a rate of 0.1 Å s$^{-1}$ through a metal shadow mask that defined a series of transistor devices with a channel length ($L$) of 50 μm and a channel width ($W$) of 1 mm. The characterization was accomplished by keithley 4200 SCS with a micromanipulator 6150 probe station in a clean shielded box at ambient atmosphere. Then field-effect mobility was calculated from the standard equation for the saturation region in metal-dioxide-semiconductor field-effect transistors: $I_{DS} = (W/2L)\mu C_i(V_G - V_T)^2$, where $I_{DS}$ is the drain-source current, $\mu$ is the field-effect mobility, $W$ and $L$ are the channel width and length, $C_i$ is the capacitance per unit area of the dielectric layer ($C_i$ = 7.5 nF cm$^{-2}$), $V_G$ is the gate voltage and $V_T$ is the threshold voltage.

## Fabrication and characterization of polymer solar cells

PSC devices were fabricated with a structure of ITO/PEDOT:PSS/**P1**:PC$_{71}$BM/Al. The patterned indium tin oxide (ITO) glass (sheet resistance 30 Ω □$^{-1}$) was precleaned in an ultrasonic bath of acetone and isopropanol and treated in an ultraviolet-ozone chamber (Jelight Company, USA) for 30 min. A thin layer (30 nm) of poly(3,4-ethylenedioxythiophene):poly(styrene sulfonate) (PEDOT:PSS, Baytron P VP AI 4083, Germany) was spin-coated onto the ITO glass and baked at 150 °C for 30 min. A chloroform solution of a blend of **P1**/PC$_{71}$BM (1 : 3 weight ratio) was subsequently spin-coated on the surface of the PEDOT:PSS layer to form a photosensitive layer. An aluminum layer (ca. 70 nm) was then evaporated onto the surface of the photosensitive layer under vacuum (ca. 10$^{-4}$ Pa). The active area of the device was 4 mm$^2$. The current–voltage curve was measured with a computer-controlled Keithley 236 Source Measure Unit. A xenon lamp coupled with AM 1.5 solar spectrum filters was used as the light source, and the optical power at the sample was 100 mW cm$^{-2}$. The external quantum efficiency (EQE) spectrum was measured using a Stanford Research Systems model SR830 DSP lock-in amplifier coupled with a WDG3 monochromator and 500 W xenon lamp.

## Synthesis

***N*-(2-decyl-tetradecyl)-2,7-dibromocarbazole (1).** To a solution of 2,7-dibromocarbazole (2 mmol, 650 mg) in 6 mL DMF was added K$_2$CO$_3$ (4 mmol, 552 mg) under a N$_2$ atmosphere. At 80 °C, 2-decyl-tetradecyl bromide (3 mmol, 1.25 g) was added slowly. The mixture was stirred at 80 °C for 16 h. After cooling to

room temperature, the organic phase was extracted with diethyl ether, and washed with H$_2$O twice. The extracts were dried over anhydrous MgSO$_4$. After removal of the solvent, the residue was purified by column chromatography on silica gel (hexanes) to give a white solid (500 mg, 38%). $^1$H NMR (400 MHz, CDCl$_3$): δ 7.86 (d, $J$ = 8.2 Hz, 2H), 7.47 (d, $J$ = 1.2 Hz, 2H), 7.31 (dd, $J$ = 8.2 Hz, $J$ = 1.4 Hz, 2H), 4.00 (d, $J$ = 7.5 Hz, 2H), 2.06 (m, 1H), 1.27–1.22 (m, 40H), 0.92 (t, $J$ = 6.8 Hz, 6H). $^{13}$C NMR (75 MHz, CDCl$_3$): δ 141.84, 122.55, 121.43, 121.25, 119.70, 112.33, 47.86, 37.62, 32.04, 32.02, 31.71, 30.00, 29.77, 29.72, 29.66, 29.49, 29.44, 26.46, 22.81, 14.25. HRMS (EI): 659.2689 (calcd for C$_{36}$H$_{55}$NBr$_2$, 659.2701). Anal. Calcd for C$_{36}$H$_{55}$NBr$_2$: C, 65.35; H, 8.38; N, 2.12. Found: C, 65.32; H, 8.42; N, 2.00%.

***N*-(2-decyl-tetradecyl)-2,7-bis(thiophen-2-yl)carbazole (2).** To a solution of **1** (1 mmol, 660 mg) and 2-tributylstannylthiophene (3 mmol, 1.12 g) in anhydrous toluene (10 mL) was added Pd(PPh$_3$)$_4$ (0.1 mmol, 115 mg) under a N$_2$ atmosphere. The mixture was stirred at 110 °C for 48 h. After cooling to room temperature, a 10 mL aqueous solution of KF (5 g) was added and the mixture was stirred for 2 h. The organic layer was extracted with CH$_2$Cl$_2$, and washed subsequently with 10% HCl aqueous solution and saturated NaHCO$_3$ aqueous solution. The extracts were dried over anhydrous MgSO$_4$. After removal of the solvent, the residue was purified by column chromatography on silica gel (CH$_2$Cl$_2$/hexanes = 1 : 5) to give a pale yellow solid (330 mg, 50%). $^1$H NMR (400 MHz, CDCl$_3$): δ 8.04 (d, $J$ = 8.1 Hz, 2H), 7.59 (s, 2H), 7.52 (dd, $J$ = 8.1 Hz, $J$ = 1.1 Hz, 2H), 7.41 (d, $J$ = 3.4 Hz, 2H), 7.32 (d, $J$ = 5.1 Hz, 2H), 7.15 (dd, $J$ = 4.8 Hz, $J$ = 3.7 Hz, 2H), 4.19 (d, $J$ = 7.2 Hz, 2H), 2.19 (m, 1H), 1.31–1.22 (m, 40H), 0.91 (t, $J$ = 6.3 Hz, 6H). $^{13}$C NMR (75 MHz, CDCl$_3$): δ 145.75, 141.91, 132.06, 128.09, 124.47, 122.92, 122.17, 120.59, 117.70, 106.22, 47.34, 37.88, 32.02, 30.05, 29.80, 29.75, 29.48, 29.46, 26.69, 22.80, 14.24. MS (MALDI): $m/z$ 667 (M$^+$). Anal. Calcd for C$_{44}$H$_{61}$NS$_2$: C, 79.10; H, 9.20; N, 2.10. Found: C, 79.22; H, 9.22; N, 2.10%.

***N*-(2-decyl-tetradecyl)-2,7-bis(5-(trimethylstannyl)thiophen-2-yl)carbazole (3).** To a solution of **2** (0.35 mmol, 234 mg) in anhydrous THF (8 mL) was added 2.5 M *n*-BuLi (0.77 mmol, 0.31 mL) in small portions at −78 °C under a N$_2$ atmosphere. After stirring for 1 h, SnMe$_3$Cl (0.77 mmol, 153.2 mg) was added; 10 min later, the mixture was warmed to room temperature, and stirred overnight. A drop of H$_2$O was added to quench the reaction, the organic phase was extracted with diethyl ether, and washed with H$_2$O twice. The extracts were dried over anhydrous MgSO$_4$. After removal of the solvent, a pale yellow semisolid was obtained (330 mg, 95%). This monomer was directly used for next reaction without further purification due to its instability. $^1$H NMR (400 MHz, CDCl$_3$): δ 8.03 (d, $J$ = 8.1 Hz, 2H), 7.59 (s, 2H), 7.52 (d, $J$ = 8.0 Hz, 2H), 7.51 (d, $J$ = 3.4 Hz, 2H), 7.22 (d, $J$ = 3.3 Hz, 2H), 4.20 (d, $J$ = 6.4 Hz, 2H), 2.17 (m, 1H), 1.43–1.22 (m, 40H), 0.89 (t, $J$ = 6.3 Hz, 6H), 0.49 (t, $J$ = 56.4, 18H).

**4,7-Dibromo-5,5′-bibenzo[c][1,2,5]thiadiazole (4).** To a suspension of BBT (2 mmol, 540 mg) in HBr aqueous solution (8 mL) was added Br$_2$ (12 mmol, 1.92 g) dissolved in 6 mL HBr aqueous solution slowly while stirring vigorously. After refluxing at 110 °C for 24 h, the mixture was cooled to room temperature,

then poured into saturated NaHSO₃ aqueous solution. The precipitate was filtered, washed with water, and dried under vacuum. The crude product was purified by column chromatography on silica gel (CH₂Cl₂/hexanes = 3 : 1) to give a dibromides mixture of BBT (256 mg, 30%). The BBT dibromides mixture could have 4 possible isomers (Figure S1,† ESI), which cannot be separated by column chromatography. Thus, the isomers mixture was treated with Br₂ in HBr solution (1 : 5 molar ratio), and refluxed for 12 h. Probably due to the dominated ratio in the mixture (Figure S3,† ESI) and relatively weaker reactivity of **4**, the isomers **4a–c** were completely converted to tri- and tetrabromide while most of **4** still remained even after reflux for 72 h. The mixture was cooled to room temperature, then poured into saturated NaHSO₃ aqueous solution. The precipitate was filtered, washed with water, and dried under vacuum. The residue was purified by column chromatography on silica gel (CH₂Cl₂/hexanes = 3 : 1) to give **4** as a yellow solid (45 mg, 17%). ¹H NMR (600 MHz, CDCl₃): $\delta$ 8.15 (m, 2H), 7.97 (s, 1H), 7.76 (dd, $J$ = 9.3 Hz, $J$ = 1.5 Hz, 1H). HRMS (EI): 427.8216 (calcd for $C_{12}H_4N_4S_2Br_2$, 427.8224). Anal. Calcd for $C_{12}H_4N_4S_2Br_2$: C, 33.67; H, 0.94; N, 13.09. Found: C, 33.81; H, 0.94; N, 13.04%.

**Poly{[N-(2-decyl-tetradecyl)-carbazole-2,7-diyl]-alt-[4,7-bis(2-thienyl)-5,5′-bibenzo[c][1,2,5]thiadiazole-5,5′-diyl]} (P1).** To a mixture of **3** (0.15 mmol, 149 mg) and **4** (0.15 mmol, 64.2 mg) in toluene (4 mL) was added Pd(PPh₃)₄ (0.01 mmol, 12 mg) under a N₂ atmosphere. The mixture was stirred at 110 °C for three days. To end-cap the polymer chain, trimethylphenylstannane (0.015 mmol, 5.5 mg) was added under nitrogen and the mixture was stirred at reflux for 10 h. Bromobenzene (0.03 mmol, 5 mg) was then added under nitrogen, and the mixture was stirred at reflux for 10 h. After the reaction mixture was cooled to room temperature, chloroform (100 mL) was added to the reaction mixture and washed with water. The organic layer was concentrated to 5 mL and dropped into methanol (200 mL). The precipitate was filtered. Finally, the polymer was purified by size exclusion column chromatography over Bio-Rad Bio-beads S-X1 eluting with chloroform to afford a black solid (120 mg, 88%). ¹H NMR (400 MHz, CDCl₃): $\delta$ 8.32 (br, 6H), 7.62 (br, 4H), 7.10 (br, 4H), 3.96 (br, 2H), 1.91 (br, 1H), 1.17 (br, 40H), 0.83 (br, 6H). Anal. Calcd for $C_{56}H_{63}N_5S_4$: C, 71.83; H, 7.00; N, 7.48. Found: C, 71.07; H, 6.97; N, 7.08%. $M_n$, 11 513; $M_w/M_n$, 2.53.

**Poly{[N-(2-decyl-tetradecyl)-carbazole-2,7-diyl]-alt-[4,7-bis(2-thienyl)-benzo[c][1,2,5]thiadiazole-5,5′-diyl]} (P2).** To a mixture of **3** (0.15 mmol, 149 mg) and 4,7-dibromobenzo[c][1,2,5] thiadiazole (0.15 mmol, 44 mg) in toluene (4 mL) was added Pd(PPh₃)₄ (0.01 mmol, 12 mg) under a N₂ atmosphere. The mixture was stirred at 110 °C for 24 h. To end-cap the polymer chain, trimethylphenylstannane (0.015 mmol, 5.5 mg) was added under nitrogen and the mixture was stirred at reflux for 10 h. Bromobenzene (0.03 mmol, 5 mg) was then added under nitrogen, and the mixture was stirred at reflux for 10 h. The reaction mixture was cooled to room temperature, and dropped into methanol (200 mL). The precipitate was filtered to give a black solid (100 mg, 83%). We did not take any purification and device fabrication and measurements due to poor solubility in common organic solvents.

## References and notes

1 N. S. Sariciftci, L. Smilowitz, A. J. Heeger and F. Wudl, *Science*, 1992, **258**, 1474.

2 (a) S. Günes, H. Neugebauer and N. S. Sariciftci, *Chem. Rev.*, 2007, **107**, 1324; (b) Y.-J. Cheng, S.-H. Yang and C.-S. Hsu, *Chem. Rev.*, 2009, **109**, 5868; (c) X. Zhan and D. Zhu, *Polym. Chem.*, 2010, **1**, 409.

3 G. Yu, J. Cao, J. C. Hummelen, F. Wudl and A. J. Heeger, *Science*, 1995, **270**, 1789.

4 (a) G. Li, V. Shrotriya, J. S. Huang, Y. Yao, T. Moriarty, K. Emery and Y. Yang, *Nat. Mater.*, 2005, **4**, 864; (b) W. L. Ma, C. Y. Yang, X. Gong, K. H. Lee and A. J. Heeger, *Adv. Funct. Mater.*, 2005, **15**, 1617.

5 (a) Y. Liang, Z. Xu, J. Xia, S.-T. Tsai, Y. Wu, G. Li, C. Ray and L. Yu, *Adv. Mater.*, 2010, **22**, E135; (b) H.-Y. Chen, J. Hou, S. Zhang, Y. Liang, G. Yang, Y. Yang, L. Yu, Y. Wu and G. Li, *Nat. Photonics*, 2009, **3**, 649; (c) H. J. Son, W. Wang, T. Xu, Y. Y. Liang, Y. Wu, G. Li and L. Yu, *J. Am. Chem. Soc.*, 2011, **133**, 1885; (d) S. C. Price, A. C. Stuart, L. Yang, H. Zhou and W. You, *J. Am. Chem. Soc.*, 2011, **133**, 4625; (e) H. Zhou, L. Yang, A. C. Stuart, S. C. Price, S. Liu and W. You, *Angew. Chem., Int. Ed.*, 2011, **50**, 2995.

6 (a) M. C. Scharber, D. Mühlbacher, M. Koppe, P. Denk, C. Waldauf, A. J. Heeger and C. J. Brabec, *Adv. Mater.*, 2006, **18**, 789.

7 (a) E. Zhou, Q. Wei, S. Yamakawa, Y. Zhang, K. Tajima, C. Yang and K. Hashimoto, *Macromolecules*, 2010, **43**, 821; (b) E. Perzon, F. Zhang, M. Andersson, W. Mammo, O. Inganäs and M. R. Andersson, *Adv. Mater.*, 2007, **19**, 3308.

8 (a) Y. Li, L. Xue, H. Li, Z. Li, B. Xu, S. Wen and W. Tian, *Macromolecules*, 2009, **42**, 4491; (b) Z.-G. Zhang, K.-L. Zhang, G. Liu, C.-X. Zhu and K.-G. Neoh, *Macromolecules*, 2009, **42**, 3104; (c) E. Wang, M. Wang, L. Wang, C. Duan, J. Zhang, W. Cai, C. He, H. Wu and Y. Cao, *Macromolecules*, 2009, **42**, 4410.

9 (a) C. Piliego, T. W. Holcombe, J. D. Douglas, C. H. Woo, P. M. Beaujuge and J. M. J. Fréchet, *J. Am. Chem. Soc.*, 2010, **132**, 7595; (b) G. Zhang, Y. Fu, Q. Zhang and Z. Xie, *Chem. Commun.*, 2010, **46**, 4997; (c) X. Zhou, L. Yang, S. Stongeking and W. You, *ACS Appl. Mater. Interfaces*, 2010, **2**, 1377; (d) X. Zhan, Z. Tan, B. Domercq, Z. An, X. Zhang, S. Barlow, Y. Li, D. Zhu, B. Kippelen and S. R. Marder, *J. Am. Chem. Soc.*, 2007, **129**, 7246; (e) X. G. Zhao and X. W. Zhan, *Chem. Soc. Rev.*, 2011, **40**, 3728.

10 (a) J. Chen and Y. Cao, *Acc. Chem. Res.*, 2009, **42**, 1709; (b) M. C. Scharber, M. Koppe, J. Cao, F. Cordella, M. A. Loi, P. Denk, M. Morana, H.-J. Egelhaaf, K. Forberich, G. Dennler, R. Gaudiana, D. Waller, Z. Zhu, X. Shi and C. J. Brabec, *Adv. Mater.*, 2010, **22**, 367.

11 (a) L. H. Slooff, S. C. Veenstra, J. M. Kroon, D. J. D. Moet, J. Sweelssen and M. M. Koetse, *Appl. Phys. Lett.*, 2007, **90**, 143506; (b) E. Wang, L. Wang, L. Lan, C. Luo, W. Zhuang, J. Peng and Y. Cao, *Appl. Phys. Lett.*, 2008, **92**, 033307; (c) J. Lu, F. Liang, N. Drolet, J. Ding, Y. Tao and R. Movileanu, *Chem. Commun.*, 2008, 5315; (d) C. P. Chen, S. H. Chan, T. C. Chao, C. Ting and T. Ko, *J. Am. Chem. Soc.*, 2008, **130**, 12828; (e) D. Mühlbacher, M. Scharber, M. Morana, Z. Zhu, D. Waller, R. Gaudiana and C. Brabec, *Adv. Mater.*, 2006, **18**, 2884; (f) J. H. Hou, H. Y. Chen, S. Q. Hang, G. Li and Y. Yang, *J. Am. Chem. Soc.*, 2008, **130**, 16144; (g) W. Yue, Y. Zhao, S. Shao, H. Tian, Z. Xie, Y. Geng and F. Wang, *J. Mater. Chem.*, 2009, **19**, 2199; (h) L. Huo, J. Hou, S. Zhang, H.-Y. Chen and Y. Yang, *Angew. Chem., Int. Ed.*, 2010, **49**, 1500.

12 M. Wang, X. Hu, P. Liu, W. Li, X. Gong, F. Huang and Y. Cao, *J. Am. Chem. Soc.*, 2011, **133**, 9638.

13 (a) J. Li, F. Dierschke, J. Wu, A. C. Grimsdale and K. Müllen, *J. Mater. Chem.*, 2006, **16**, 96; (b) N. Leclerc, A. Michaud, K. Sirois, J. F. Morin and M. Leclerc, *Adv. Funct. Mater.*, 2006, **16**, 1694.

14  N. Blouin, A. Michaud, D. Gendron, S. Wakim, E. Blair, R. Neagu-Plesu, M. Belletête, G. Durocher, Y. Tao and M. Leclerc, *J. Am. Chem. Soc.*, 2008, **130**, 732.

15  N. Blouin, A. Michaud and M. Leclerc, *Adv. Mater.*, 2007, **19**, 2295.

16  (*a*) S. H. Park, A. Roy, S. Beaupré, S. Cho, N. Coates, J. S. Moon, D. Mose, M. Leclerc, K. Lee and A. J. Heeger, *Nat. Photonics*, 2009, **3**, 297; (*b*) N. Blouin and M. Leclerc, *Acc. Chem. Res.*, 2008, **41**, 1110.

17  R. Qin, W. Li, C. Li, C. Du, C. Veit, H.-F. Schleiermacher, M. Andersson, Z. Bo, Z. Liu, O. Inganäs, U. Wuerfel and F. Zhang, *J. Am. Chem. Soc.*, 2009, **131**, 14612.

18  R. Neidlein, D. Droste-Tran-Viet, A. Gieren, M. Kokkinidis, R. Wilckens, H.-P. Geserich and W. Ruppel, *Helv. Chim. Acta*, 1984, **67**, 574.

19  A. D. Becke, *J. Chem. Phys.*, 1993, **98**, 5648.

20  C. T. Lee, W. T. Yang and R. G. Parr, *Phys. Rev. B*, 1988, **87**, 785.

21  *Gaussian 09, Revision A.1*, M. J. Frisch, G. W. Trucks, H. B. Schlegel, G. E. Scuseria, M. A. Robb, J. R. Cheeseman, G. Scalmani, V. Barone, B. Mennucci, G. A. Petersson, H. Nakatsuji, M. Caricato, X. Li, H. P. Hratchian, A. F. Izmaylov, J. Bloino, G. Zheng, J. L. Sonnenberg, M. Hada, M. Ehara, K. Toyota, R. Fukuda, J. Hasegawa, M. Ishida, T. Nakajima, Y. Honda, O. Kitao, H. Nakai, T. Vreven, J. A. Montgomery, Jr., J. E. Peralta, F. Ogliaro, M. Bearpark, J. J. Heyd, E. Brothers, K. N. Kudin, V. N. Staroverov, R. Kobayashi, J. Normand, K. Raghavachari, A. Rendell, J. C. Burant, S. S. Iyengar, J. Tomasi, M. Cossi, N. Rega, J. M. Millam, M. Klene, J. E. Knox, J. B. Cross, V. Bakken, C. Adamo, J. Jaramillo, R. Gomperts, R. E. Stratmann, O. Yazyev, A. J. Austin, R. Cammi, C. Pomelli, J. W. Ochterski, R. L. Martin, K. Morokuma, V. G. Zakrzewski, G. A. Voth, P. Salvador, J. J. Dannenberg, S. Dapprich, A. D. Daniels, Ö. Farkas, J. B. Foresman, V. J. Ortiz, J. Cioslowski and D. J. Fox, Gaussian, Inc., Wallingford CT, 2009.

22  J. E. Anthony, A. Facchetti, M. Heeney, S. R. Marder and X. W. Zhan, *Adv. Mater.*, 2010, **22**, 3876.

23  (*a*) A. Salleo, R. J. Kline, D. M. Delongchamp and M. L. Chabinyc, *Adv. Mater.*, 2010, **22**, 3812; (*b*) A. J. Moulé and K. Meerholz, *Adv. Funct. Mater.*, 2009, **19**, 3028.

This journal is © The Royal Society of Chemistry 2012

*J. Mater. Chem.*, 2012, **22**, 3432–3439 | 3439